NEOPLASIA
www.neoplasia.com

Volume 17 Number 12 December 2015 pp. 849–861 **849**

# Breast Cancer Cell Colonization of the Human Bone Marrow Adipose Tissue Niche[1]

**Zach S. Templeton[*], Wen-Rong Lie[†], Weiqi Wang[‡], Yael Rosenberg-Hasson[‡], Rajiv V. Alluri[*], John S. Tamaresis[§], Michael H. Bachmann[*], Kitty Lee[¶], William J. Maloney[#], Christopher H. Contag[*] and Bonnie L. King[*]**

[*]Department of Pediatrics, 150E Clark Center, 318 Campus Drive, Stanford University School of Medicine, Stanford, CA 94305-5427; [†]EMD Millipore Corporation, 14 Research Park Drive, St Charles, MO 63304-5618; [‡]Department of Immunology, Fairchild Science Building, D033, 299 Campus Drive, Stanford University School of Medicine, Stanford, CA 94305-5124; [§]Department of Biomedical Data Science, Room T101F, Redwood Building, 150 Governor's Lane, Stanford University School of Medicine, Stanford, CA 94305-5405; [¶]Cell Sciences Imaging Facility, Beckman Center (B050B), Stanford University School of Medicine, Stanford, CA 94305-5301; [#]Department of Orthopaedic Surgery, 450 Broadway Street, Pavillion C, 4th Floor, Stanford University School of Medicine, Redwood City, CA 94063-6342

## Abstract

*BACKGROUND/OBJECTIVES:* Bone is a preferred site of breast cancer metastasis, suggesting the presence of tissue-specific features that attract and promote the outgrowth of breast cancer cells. We sought to identify parameters of *human* bone tissue associated with breast cancer cell osteotropism and colonization in the metastatic niche. *METHODS:* Migration and colonization patterns of MDA-MB-231-fLuc-EGFP (luciferase-enhanced green fluorescence protein) and MCF-7-fLuc-EGFP breast cancer cells were studied in co-culture with cancellous bone tissue fragments isolated from 14 hip arthroplasties. Breast cancer cell migration into tissues and toward tissue-conditioned medium was measured in Transwell migration chambers using bioluminescence imaging and analyzed as a function of secreted factors measured by multiplex immunoassay. Patterns of breast cancer cell colonization were evaluated with fluorescence microscopy and immunohistochemistry. *RESULTS:* Enhanced MDA-MB-231-fLuc-EGFP breast cancer cell migration to bone-conditioned versus control medium was observed in 12/14 specimens ($P = .0014$) and correlated significantly with increasing levels of the adipokines/cytokines leptin ($P = .006$) and IL-1β ($P = .001$) in univariate and multivariate regression analyses. Fluorescence microscopy and immunohistochemistry of fragments underscored the extreme adiposity of adult human bone tissues and revealed extensive breast cancer cell colonization within the marrow adipose tissue compartment. *CONCLUSIONS:* Our results show that breast cancer cells migrate to human bone tissue-conditioned medium in association with increasing levels of leptin and IL-1β, and colonize the bone marrow adipose tissue compartment

Address all correspondence to: Bonnie L. King, Ph.D., Department of Pediatrics, 150E Clark Center, 318 Campus Drive, Stanford University School of Medicine, Stanford, CA 94305-5427.
E-mail: bonnie.king@stanford.edu

[1] These studies were funded, in part, by grants from the Alternative Research and Development Foundation (107588), the National Institutes of Health (5R01CA172895-02), and the California Breast Cancer Research Program (201B-0141) and generous support from the Chambers Family Foundation. This work was also supported, in part, by the National Institutes of Health (P30CA124435) using the following Stanford Cancer Institute Shared Resources: Human Immune Monitoring Shared Resource, Cell Sciences Imaging Shared Resource, and Biostatistics and Research Informatics Shared Resource.
Received 27 September 2015; Revised 5 November 2015; Accepted 10 November 2015

© 2015 The Authors. Published by Elsevier Inc. on behalf of Neoplasia Press, Inc. This is an open access article under the CC BY-NC-ND license (http://creativecommons.org/licenses/by-nc-nd/4.0/).
1476-5586
http://dx.doi.org/10.1016/j.neo.2015.11.005

of cultured fragments. Bone marrow adipose tissue and its molecular signals may be important but understudied components of the breast cancer metastatic niche.

*Neoplasia (2015) 17, 849–861*

## Introduction

Breast cancer metastasis is responsible for most breast cancer mortality. The process unfolds when epithelial cells lining the mammary tree traverse the surrounding basement membrane and invade the collagenous stroma populated by fibroblasts, adipocytes, and infiltrating immune cells to access vasculature conveying passage to distant organs. Although breast cancer commonly spreads to lung, brain, and liver, the most prevalent site of breast cancer metastasis is bone [1,2]. This organ-specific metastatic pattern has long been explained by Paget's seed and soil hypothesis, which postulates that the microenvironment of certain organs attracts and promotes the growth of specific types of cancer cells [3]. Bone-seeking malignancies include breast and prostate cancers, suggesting the presence of bone-specific factors that attract and promote colonization of these but not all metastatic cancers [2]. An alternate explanation, posited by Ewing, proposes that permissive features of the target organ microvasculature facilitate specific metastatic patterns [4]. Breast cancer metastasis to bone occurs most frequently throughout the axial skeleton, which is populated by "red marrow" where active hematopoiesis requires continuous passage of cells into the circulation [5,6]. As such, sinusoids that permit the exit of cells during hematopoiesis may facilitate the enhanced entry of circulating tumor cells to colonize the bone marrow. However, not all metastatic cancers spread to the bone, indicating that access alone may be insufficient. Thus, although circulatory parameters may facilitate enhanced access to certain organs, it appears that other properties must be responsible for migration into and colonization of the metastatic niche.

To date, a number of different isolated bone cell types have been evaluated for their ability to recruit breast cancer cells, including osteoblasts; osteoclasts; mesenchymal stem cells; fibroblasts; and, most recently, adipocytes [7–17]. These studies have implicated numerous factors in breast cancer cell osteotropism, including SDF-1, CTACK, RANKL, OPG, OPN, PDGF-AB/BB, VEGF, IL-6, IL-8, GM-CSF, G-CSF, ENA-78, and 6Ckine [7,9–16]. In addition, animal model studies of bone-seeking malignancies have revealed specific areas within the bone microenvironment believed to host early colonization events [18], leading to the proposal of specific metastatic niches, including the hematopoietic stem cell niche [19]; the perivascular niche [20]; and, most recently, the osteogenic niche [21]. However, although the role of the microenvironment in cancer progression is widely acknowledged [22–24], a potentially important breast cancer metastatic niche within the bone has been understudied. The mature human skeleton, which is a frequent target of breast cancer metastasis, becomes increasingly populated by adipose tissue with age [25–27]. Although recent studies have revealed a central role for bone marrow adipose tissue in prostate cancer progression [28], relatively little attention has been paid to the potential role of bone marrow adipose tissue in breast cancer cell osteotropism and colonization events. We previously established a human bone tissue co-culture model for studying breast cancer cell behavior within the native three-dimensional microenvironment of the aging human skeleton [29,30]. In this study, we sought to identify parameters of the human bone tissue microenvironment associated with breast cancer cell migration and colonization events. Our observations underscore the extreme adiposity of the mature human skeleton and reveal robust breast cancer cell infiltration of the bone marrow adipose tissue compartment.

## Methods

### *Human Femur Tissue*

Femoral heads were collected from 14 patients undergoing elective total hip replacement (THR) in the Department of Orthopaedic Surgery at the Stanford University Medical Center over a period of 6 months. Specimens were collected from 8 female and 6 male patients ranging from 42 to 89 years of age (average = 63; median = 59). All tissues were collected as deidentified specimens in accordance with regulations of the Stanford University Research Compliance Office. Per HIPAA regulations, the exact age of the one specimen in our study isolated from an individual over the age of 89 was unknown but was estimated as 89 years for statistical calculations. Discarded femoral head specimens were placed in physiological saline, transported to the laboratory immediately following surgery, and placed into a Pyrex dish (VWR, Radnor, PA). Using a sterile glove to hold the femoral head with one hand, cancellous bone fragments measuring ~3 to 5 $mm^2$ were dissected from the shaft using a surgical Rongeur (Fine Science Tools, Foster City, CA) for placement into migration chambers and culture dishes as described previously [29,30].

### *Breast Cancer Cell Lines*

MDA-MB-231, MCF-7, and SKBR3 breast cancer cell lines and MCF-10A breast cells were purchased from the American Type Culture Collection (Rockville, MD) and engineered for the stable expression of firefly luciferase with the Sleeping Beauty transposon plasmid pKT2/LuBiG and the transposase plasmid pK/hUbiC-SB11 [31,32]. The resulting transfected cell lines are referred to as MDA-MB-231-fLuc-EGFP, MCF-7-fLuc-EGFP, SKBR3-fLuc-EGFP, and MCF-10A-fLuc-EGFP. All cell lines tested negative for mycoplasma using the MycoAlert Mycoplasma Detection Kit (Lonza, Rockland, ME).

### *Direct Seeding of Breast Cancer Cells onto Bone Tissue Fragments to Image Colonization Patterns by Fluorescence and Confocal Microscopy*

Bone fragments measuring ~3 mm in diameter were placed into the empty wells of a 24-well tissue culture plate (1 fragment/well). Cell suspensions delivering $1 \times 10^3$ to $1 \times 10^6$ MDA-MB-231-fLuc-EGFP or MCF-7-fLuc-EGFP cells in 10-µl volumes of DMEM-10% FBS were pipetted directly onto the top of each bone fragment. After all fragments were seeded, the plate was incubated in a humidified 37°C tissue culture incubator with 5% $CO_2$ for 45 minutes to promote cell attachment. Once cells attached, 1 to 2 ml of

DMEM-10% FBS was added to each well to submerge the fragments for culture in a 37°C tissue culture incubator. After 24 hours of culture, 5 µl of OsteoSense 680 (PerkinElmer) was added to each well to achieve a concentration of 1.6 nmol/2 ml of culture medium to label the mineralized trabeculae of the bone fragments, after which the plates were incubated in a 37°C tissue culture incubator for an additional 24 hours. For fluorescence microscopy at 48 hours, fragments were transferred to a 24-well tissue culture plate containing 1 ml of FluoroBrite DMEM (Life Sciences)-10% FBS/well and imaged with an epifluorescence microscope (EVOS, Life Technologies) configured to detect EGFP at 488-nm and Osteosense at 680-nm excitation wavelengths, respectively. For confocal microscopy, the fragments were incubated in a mixture of 10 ml of FluoroBrite DMEM-10% FBS and 0.2 ml of Oil Red stock solution (3 mg/ml in 100% isopropanol) for 1 hour and then transferred to FluoroDishes (World Precision Instruments) containing fresh FluoroBrite DMEM-10% FBS for imaging on an SP8 confocal microscope configured to detect EGFP at 488-nm, and Oil Red O and Osteosense at 680-nm excitation wavelengths, respectively. Z stacks were acquired at 20 × magnification and rendered into 3-dimensional images using Volocity 3D Image Analysis Software (PerkinElmer).

### *Culture of Bone Marrow Adipocytes*

Bone marrow was isolated from cancellous bone tissues by flushing individual fragments with 10-ml volumes of PBS expelled from a syringe fitted with a 25-guage needle and filtering the effluent through 70-µm strainers seated into 50-ml conical tubes. The resulting marrow cell suspensions were centrifuged for 3 minutes at room temperature at 300 ×*g*. Pellets were resuspended in ROCK medium [33] and transferred to 24-well tissue culture plates.

### *Immunohistochemical Analysis*

Bone tissue fragments were fixed in 10% buffered formalin, decalcified, and processed for paraffin embedding and slide preparation. Tissue sections were stained with hematoxylin and eosin or processed for immunohistochemical analysis using a monoclonal mouse anti-human cytokeratin antibody (Clone AE1/AE3) (Dako Cytomation, Carpenteria, CA).

### *Generation of Bone Tissue Culture Supernatants for Migration Assays and Secretome Analysis*

Three fragments from each THR specimen were used to generate bone tissue culture supernatants for use in migration assays and secretome analysis. Bone tissue fragments were transferred into 3 separate wells of a 12-well tissue culture plate containing 2.2 ml of DMEM-10% FBS per well. Three control wells received equivalent volumes of medium but no fragments. Plates were incubated for 24 hours at 37°C. At 24 hours, the medium was removed and replenished for all tissue-containing and control wells, followed by an additional 24 hours of incubation. At 48 hours, 0.9- and 1-ml aliquots of medium were collected from all wells for use in migration and secretome analyses respectively.

### *Migration Assays*

Transwell permeable cell culture inserts with 8-µm pores (Corning Incorporated Life Sciences, Tewksbury, MA) were used for two different types of migration assays [30]. In the first type of assay, using a nontraditional "reverse" migration protocol illustrated in Figure 3*A*, the cell culture inserts were placed upside down to be seeded with breast cancer cell suspensions ($1 \times 10^5$ luciferase-positive breast cancer cells per 50 µl) onto the bottom surfaces of the insert cups. The seeded cups were incubated at 37°C, 5% $CO_2$ for 45 minutes to promote cell attachment, after which they were turned right side up for placement into the wells of a 24-well tissue culture plate (MULTIWELL, Becton Dickinson, Franklin Lakes, NJ) containing 0.9 ml DMEM-10% FBS/well. Single bone tissue fragments measuring ~3 mm in diameter or control glass beads were placed into individual seeded inserts, which were then submerged in 450 µl of DMEM-10% FBS/well. Migration plates were incubated at 37°C, 5% $CO_2$ for 24 h, after which the bone fragments and control glass beads were transferred into DMEM-10% FBS–containing wells of a fresh 24-well tissue culture plate to assess the presence of bioluminescence signal (Figure 3, *B* and *C*). In the second type of assay (using a traditional protocol) diagrammed in Figure 4*A*, 350 µl of DMEM-10% FBS containing $1 \times 10^5$ luciferase-positive breast cancer cells were seeded onto the upper surfaces of insert cups seated in an empty standard 24-well tissue culture plate and then incubated at 37°C, 5% $CO_2$ for 45 minutes to promote cell attachment. Seeded inserts were then transferred to a MULTIWELL 24-well tissue culture plate containing 0.9 ml of THR supernatant or control DMEM-10% FBS medium per well. Migration plates were incubated at 37°C, 5% $CO_2$ for 20 hours, after which the inserts were removed from all wells (Figure 4*B*). Once the inserts were removed, the receiver plate was imaged with an IVIS imaging system (Xenogen Product of Perkin Elmer, Waltham, MA) to detect cells that migrated and attached to the bottom of each well (Figure 4*C*). Each experimental sample (bone supernatants or fragments from a given THR specimen, or control medium) was tested in triplicate.

### *Bioluminescence Imaging*

Bioluminescence imaging (BLI) was performed on cells and tissues following migration experiments in an IVIS 50 Imaging Platform (Xenogen Product of Perkin Elmer, Waltham, MA) immediately following addition of D-luciferin substrate (150 µg/ml) to all wells. Imaging parameters were F-stop of 1, small binning, level D, and exposure time of 30 seconds. The signal intensities are reported as average radiance (photons/s per $cm^2$ per sr). Average radiance was integrated over individual wells designated as regions of interest using the Living Image Software Program (Version 4.3.1. Perkin Elmer).

### *Statistical Analysis of Breast Cancer Cell Migration to Bone Fragments versus Glass Beads, and Bone-Conditioned versus Control Medium*

The migration of MDA-MB-231-fLuc-EGFP cells to triplicate sets of wells containing bone tissue fragments versus control glass beads was evaluated across 14 THR specimens by measuring the presence versus absence of bioluminescence signal in each well. Comparison of the numbers of signals in wells with bone fragments versus glass beads was analyzed using a two-sided Fisher's exact test. The migration of MDA-MB-231-fLuc-EGFP cells to triplicate wells containing bone tissue supernatant versus control medium was quantified across 14 THR specimens using BLI and expressed as average radiance (photons/s per $cm^2$ per sr). For the purpose of statistical analysis, the average radiance values were transformed by taking natural logarithms. We tested the null hypothesis that the mean log-transformed radiance values do not differ between the averaged bone-conditioned supernatant and control medium wells using the

*t* test applied to replicate-averaged data and the within-subjects one-way analysis of variance applied to replicated data.

### *Bone Tissue Fragment Secretome Analysis*

Multiplex immunoassays of 75 protein analytes including cytokines, growth factors, and adipokines were performed on the cultured bone tissue fragment supernatants and control media generated in triplicate for migration assays performed across 14 of the THR specimens. One-milliliter volumes of bone tissue fragment-conditioned medium or DME-10% FBS control medium from all wells were collected into microfuge tubes and centrifuged for 5 minutes at 13,000 rpm on a tabletop microcentrifuge at room temperature. Supernatants from these centrifugations were stored at −80°C until analysis using MILLIPLEX MAP magnetic bead immunoassay kits (EMD Millipore, Billerica, MA) based on the Luminex xMAP technology. Levels of analytes were quantitatively measured using MILLIPLEX MAP Human Cytokine/Chemokine Panels I and II, Human Bone Panel, and RANKL (EMD Millipore, Billerica, MA) as per the manufacturer's instructions. Duplicate aliquots of each supernatant sample were evaluated for each biomarker. In brief, 25 µl of supernatant and control samples (or standards) was incubated with 25 µl of magnetic beads conjugated with capture antibodies in a 96-well plate overnight at 4°C. On day 2, the beads were washed, 25 or 50 µl biotinylated detection antibody cocktail was added, and the assay plates were incubated at room temperature for 1 hour. Then, 25 µl of streptavidin-phycoerythrin was added for a further 30-minute incubation. The beads were then washed and resuspended in 100 µl buffer to read fluorescence levels on a Luminex 200 Instrument. Fluorescence levels generated in the sample data set were expressed as median fluorescence intensity (MFI). MFI data were used for subsequent analyses based on two considerations: 1) our choice of bone tissue culture supernatant volumes was arbitrary, and 2) matrix effects result in an approximation of concentration [34]. The standard curves offer a semiquantitative normalization method. Because our intent was to determine the association between migration and analyte levels, we employed the raw MFI data [35].

### *Statistical Analysis of Migration as a Function of Biomarker Levels*

To evaluate MDA-MB-231-fLuc-EGFP breast cancer cell migration to bone tissue supernatants as a function of analyte levels, BLI signal (reflecting migration) was analyzed as a function of MFI signal (reflecting analyte concentration) across triplicate samples from 13 THR specimens (THRs 44-56) by regression analysis using linear mixed models. (THR 43 supernatants were used for pilot immunoassay protocol development and thus were not included in statistical analyses.) More specifically, the ratios (fold increase) of BLI signals detected in migration assays for conditioned versus control medium were analyzed as a function of the ratios of MFI signal for analytes in the same samples. Log-transformed values were used for all statistical tests. R (R Core Team, 2012) and the software tool lme4 package in R v3.1.2 were used to perform a linear mixed effects analysis of the relationship between BLI and analyte MFI ratios [36,37]. We entered analyte MFI ratios and plate IDs (to account for batch effects) into the model as fixed effects and intercepts for patients as random effects. Univariate regression analysis [with and without adjustment for age, gender, and false discovery rate (FDR) ($q = 0.05$)] was performed on all 75 analytes interrogated by the 4 MILLIPLEX MAP panels. Coefficients and *P* values for this analysis are listed in Supplementary Table 1. In addition, multivariate regression analysis (including age and gender as covariates) was performed to test the association of five of the analytes interrogated by the MILLIPLEX MAP Human Bone Panel (leptin, IL-1β, IL-6, OPG, OPN) with breast cancer cell migration. All *P* values were two-tailed.

## Results

### *THR Specimens*

Fourteen femoral head specimens were collected as discarded tissues following total hip replacement surgeries performed in the Department of Orthopaedic Surgery at the Stanford University School of Medicine over a period of 6 months. Bone specimens were collected from male and female patients to survey the full spectrum of properties potentially underlying the progression of bone-seeking malignancies, which also occur in the male skeleton (e.g., prostate cancer). All femoral heads included a portion of the proximal femur, containing cancellous bone tissue (Figure 1*A*), the color of which varied from red to yellow across patient specimens, as illustrated by the fragments shown in Figure 1*B*. The cancellous tissue fragments, isolated from individuals ranging from 42 to 89 years of age, consistently harbored copious amounts of adipose tissue, as revealed by histology (Figure 1*C*), fluorescence microscopy (Figure 1*D*), the production of fat micelles during explant culture (Figure 1*E*), and the robust outgrowth of adipocytes from cultured bone marrow cells (Figure 1*F*). These qualitative observations illustrate the extreme adiposity of the mature human bone marrow compartment.

### *Patterns of Breast Cancer Cell Colonization*

During 48 hours of co-culture following direct seeding of breast cancer cells onto tissue fragments, breast cancer cells colonized the mineralized and marrow compartments of the trabecular bone fragments. Fluorescence microscopy revealed extensive infiltration of MDA-MB-231-fLuc-EGFP and MCF-7-fLuc-EGFP cells into the marrow compartment, where they displayed direct, extensive contact with adipocytes (Figure 2*A*). Postculture immunohistochemistry confirmed the presence of cytokeratin-positive MCF-7-fLuc-EGFP cells surrounding adipocytes in fixed bone tissues (Figure 2*B*). Confocal microscopy further illustrated the extensive, direct contacts between MCF-7-fLuc-EGFP breast cancer cells and adipocytes in bone fragments stained with Oil Red, revealing breast cancer cell psuedopodial extensions around adjacent adipocytes (Figure 2, *C* and *D*; Supplemental Data Video 1). Although our qualitative observations revealed breast cancer cell contacts with bone cells throughout the mineralized and marrow compartments, they exhibited preferential, directed migration toward adipocytes. These patterns of colonization reveal extensive breast cancer cell infiltration of the bone marrow adipose tissue compartment and direct contact between breast cancer cells and adipocytes.

### *Breast Cancer Cell Line Migration to Bone Tissue Fragments*

MDA-MB-231-fLuc-EGFP cells migrated through microporous membranes to colonize bone fragments as illustrated in Figure 3, *A* and *B*. Colonization following migration was detected with BLI following transfer of fragments and beads to wells containing fresh medium, as illustrated in Figure 3*C*. Migration was significantly greater to bone tissue fragments (15/42) compared with control glass beads (3/42) as determined by the Fisher's exact test ($P = .003$), with

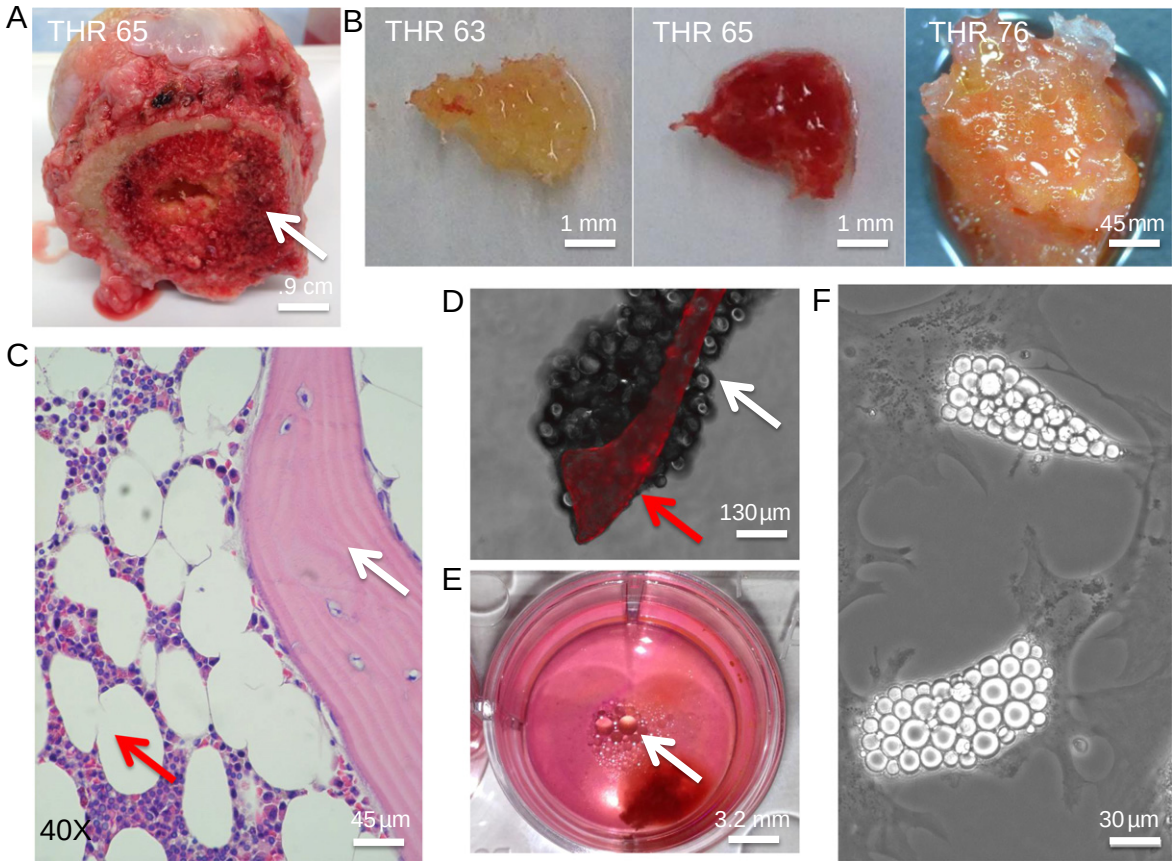


**Figure 1.** Adipose tissue is a prominent component of the mature human bone microenvironment and is accessible for study in a tissue explant model. (A) Femoral head removed during total hip replacement surgery (THR 65), with arrow pointing to cancellous bone tissue in the proximal femur. (B) Cancellous bone tissue fragments isolated from three different femoral head surgical specimens (THRs 63, 65, and 76) revealing variation in yellow versus red marrow content. (C) Histologic section of cancellous bone tissue fragment stained with hematoxylin and eosin reveals abundant adipocyte "ghosts" (red arrow) within the marrow compartment next to a mineralized bone spicule (white arrow). (D) Fluorescence image of a cancellous bone tissue spicule labeled with Osteosense 680 (red arrow) and surrounded by adipocytes (white arrow). (E) Fat micelles released into the medium of a cultured bone tissue fragment (white arrow). (F) Adipocytes isolated from bone fragment marrow growing in culture.

an odds ratio of 0.1385 and 95% confidence interval of 0.0365 to 0.5252. The viability of breast cancer cells within colonized fragments following migration was previously demonstrated by culturing the flushed marrows from BLI-positive fragments to demonstrate the subsequent outgrowth of MDA-MB-231-fLuc-EGFP cells [30]. Breast cancer cell colonization of one or more bone tissue fragments from 11/14 of the THR specimens was observed, as shown in Figure 3*D*. These results demonstrate osteotropic behavior of MDA-MB-231-fLuc-EGFP breast cancer cells for human bone tissue fragments.

### *Breast Cancer Cell Line Migration to Bone Culture Supernatants*

Comparison of migration patterns through microporous membranes revealed that MDA-MB-231-fLuc-EGFP cells, but not MCF-7-fLuc-EGFP, SKBR3-fLuc-EGFP, and MCF10A-fLuc-EGFP breast cancer cells, exhibited significantly greater migration toward bone tissue-conditioned medium versus control medium as shown in Figure 4*D* ($P < .01$). These patterns are consistent with other *in vitro* and *in vivo* studies demonstrating highly robust migration and metastatic behavior of MDA-MB-231-fLuc-EGFP cells relative to other breast cancer cell lines [12,38]. Thus, although ER-positive breast cancer cells effectively colonize the skeleton and are responsible for most late breast cancer recurrence, MDA-MB-231-fLuc-EFGP cells were used for subsequent migration assays in this study. Quantitative BLI analysis of MDA-MB-231-fLuc-EFGP migration to bone culture supernatants generated from 14 hip replacement specimens demonstrated that MDA-MB-231-fLuc-EFGP migration was greater toward bone-conditioned medium versus control medium in 12/14 specimens ($P = .0014$), as illustrated in Figure 5*A*, but varied across specimens. Fold increase in BLI signal associated with migration to conditioned versus control medium ranged from 0.75 to 3.5× (Figure 5*B*) across the 14 THR specimens analyzed. These results demonstrate that MDA-MB-231-fLuc-EFGP cell migration was consistently greater to bone-conditioned medium relative to control medium and that the magnitude of this increase varied across the 14 specimens.

### *Breast Cancer Cell Migration as a Function of Bone Tissue Secretome*

To determine if levels of secreted factors present in bone-conditioned medium were associated with MDA-MB-231-fLuc-EGFP migration patterns, we used linear mixed model regression

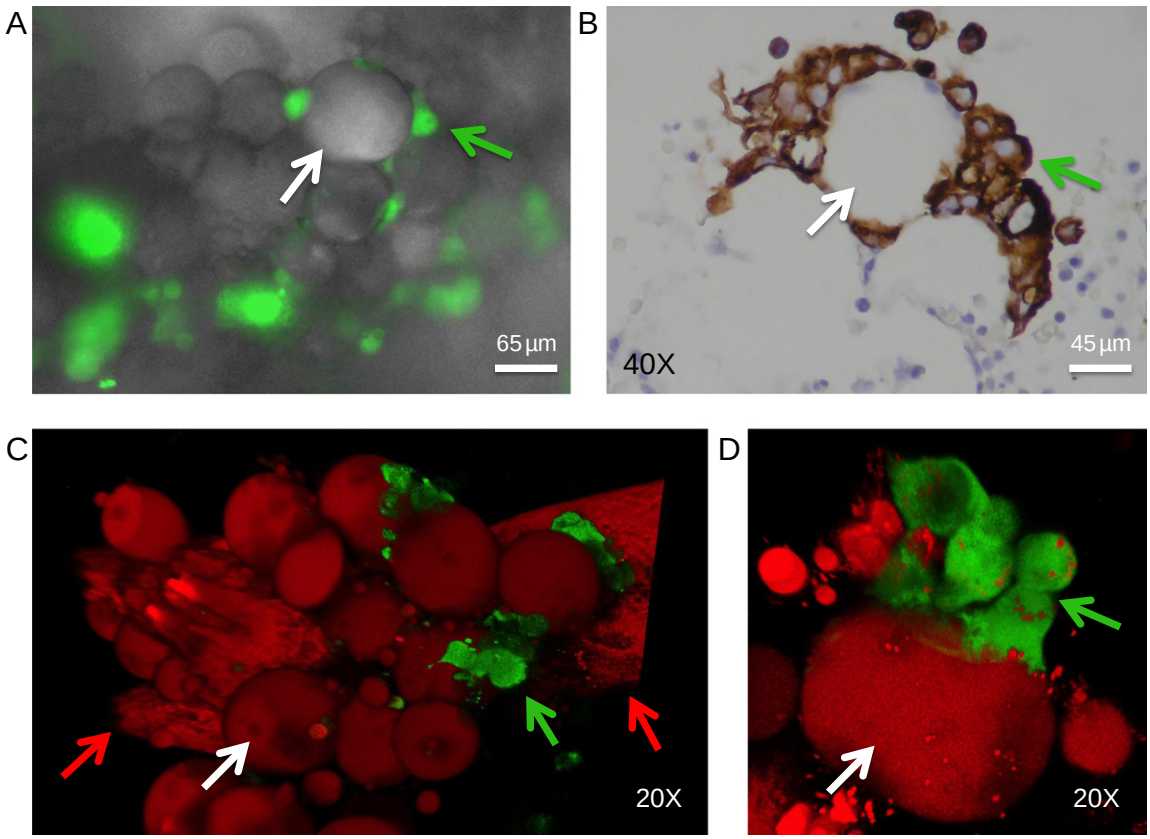


**Figure 2.** Breast cancer cells establish direct contact with adipocytes during colonization of the bone marrow compartment when co-cultured with cancellous human bone tissue fragments. (A) Fluorescence image of a cancellous bone tissue fragment seeded with MCF-7-fLuc-EGFP cells (green arrow) shown in direct contact with adipocytes (white arrow) at 24 hours. (B) Post co-culture immunohistochemical staining with AE1/3 anti-cytokeratin antibody detecting MCF-7-fLuc-EFGP cell colonization (green arrow) adjacent to adipocytes (white arrow). (C) Confocal microscopy of co-cultures at 48 hours following staining with Oil Red to define adipocytes (white arrow) and Osteosense 680 to define bone spicules (red arrow). A video of the image in panel (C) is provided in Supplementary Data Video 1. (D) MCF-7-fLuc-EGFP cells (green arrow) are shown in direct contact with adipocyte (white arrow).

analysis. Specifically, univariate regression analysis was performed on triplicate supernatant samples from 13 THR specimens to analyze migration as a function of all 75 analytes measured in our multiplex immunoassay (Supplementary Data Table 1). After controlling for age, gender, and FDR, increasing levels of 16 factors were significantly associated ($P < .05$) with MDA-MB-231-fLuc-EFGP migration: leptin, IL-1β, IL-1α, MCP-3, TNFα, IL-17A, TGFα, MIP-1β, IL-13, IL-10, GM-CSF, fractalkine, CD40L, TRAIL, IL-20, and I-309. Decreasing levels of three factors were significantly associated with migration: SOST, ACTH, and RANKL. These results confirm previously published findings suggesting that a broad constellation of secreted factors from many bone cell types participates in the recruitment of breast cancer cells into the bone microenvironment.

Because of the limited sample size of 13 THR specimens and collinearity issues associated with analyzing high numbers of analytes from multiple multiplex panels, we were not able to perform multivariate regression analysis on all 75 analytes. Thus, multivariate regression analysis was performed on a limited group of analytes of interest interrogated by a single immunoassay kit panel. Given the high level of adiposity observed in the bone fragments and the observed infiltration of breast cancer cells into the bone marrow adipose compartment over the course of our studies, we were particularly interested in the role of the adipokine leptin. In addition, a recent report identifying MDA-MB-231 breast cancer cell expression of IL-1β as a determinant of bone homing in a mouse model [39] led us to focus our attention on this analyte, which is also secreted by adipocytes. As such, we performed our multivariate regression analysis of migration patterns on a subset of adipokines and cytokines interrogated by the MILLIPLEX MAP Human Bone Panel magnetic bead immunoassay kit: leptin, IL-1β, and three other bone-secreted factors previously implicated in breast cell osteotropism (IL-6, OPG, and OPN) [9,12]. Of these factors, increasing levels of leptin and IL-1β were significantly associated with migration (before and after adjustment for age and gender) in both univariate regression ($P < .0001$) and multivariate regression analysis ($P = .006$ and $P = .001$, respectively). Scatter plots displaying migration patterns as a function of increasing levels of each factor are shown in Figure 6*A*, with regression coefficients and associated $P$ values listed in Figure 6*B*. These results reveal that increasing levels of leptin and IL-1β in human bone tissue-conditioned medium promote breast cancer cell migration.

## Discussion

In this study, we employed a human bone tissue explant model representing the aging skeleton, which is frequently the target of

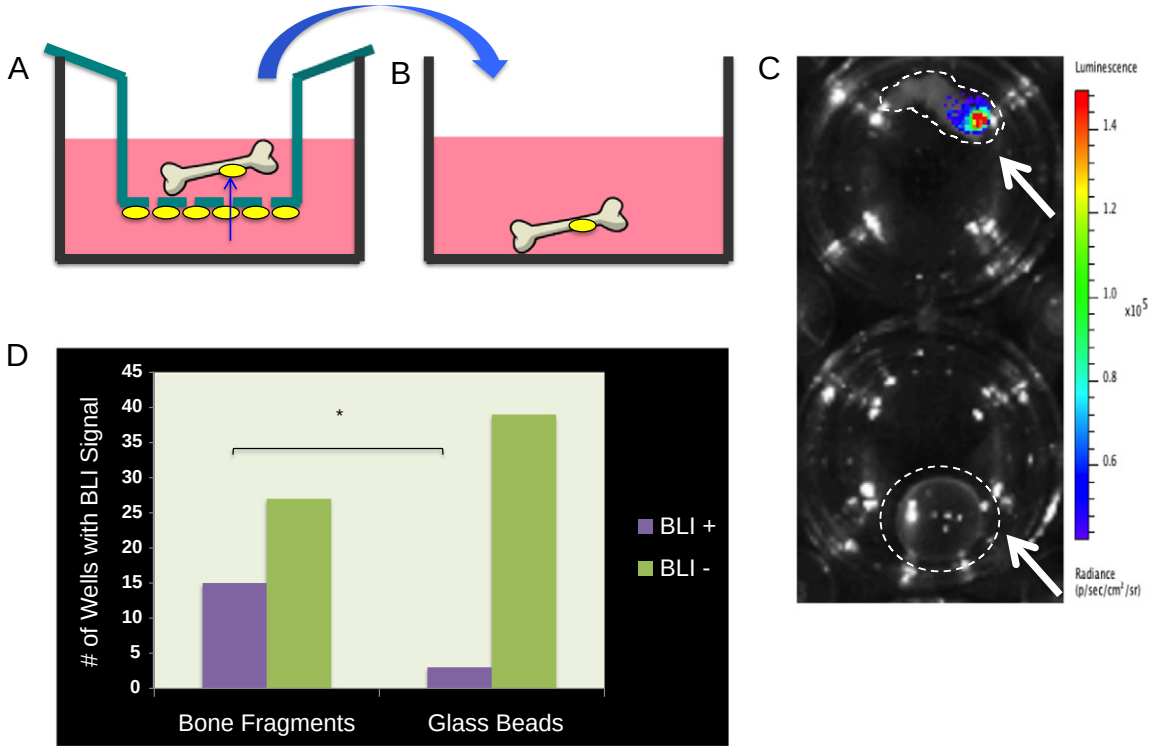


**Figure 3.** Breast cancer cells migrate through microporous membranes to human bone tissue fragments. (A) Nontraditional "reverse" migration assay design showing MDA-MB-231-fLuc-EGFP cells seeded onto the lower surface of an insert with an 8-$\mu$m porous membrane, through which they migrate to colonize a bone tissue fragment or a control glass bead. (B) Following colonization, fragments and glass beads are transferred to fresh culture wells at 24 h. (C) BLI detects breast cell colonization of bone fragment but not glass bead at 24 h. (D) Histogram showing the number of tissue fragments and glass beads with versus without bioluminescence signal. Experiments were performed in triplicate ($n$ = 3 fragments and 3 beads) for each of 14 THR specimens. Signal was observed in a significantly greater number of bone tissue fragments (15/42) versus glass beads (3/42) ($^*P$ = .003).

breast cancer metastasis, to study patterns of breast cancer cell migration and colonization. The cancellous tissues used in this culture system were isolated from the proximal femur region of femoral heads discarded following hip replacement surgeries. The proximal femur is a frequent site of breast cancer metastasis and harbors metabolically active red marrow typically targeted by metastatic spread to the skeleton [5,6,40]. Hip replacement procedures are most commonly performed in individuals aged 50 to 80 years, an age range that brackets the years of peak breast cancer incidence. In our culture system, bone tissues are maintained as intact three-dimensional fragments that retain both the mineralized spicules and marrow compartment with all potentially relevant cell types. As such, these tissues represent the microenvironment in which breast cancer metastasis unfolds within the skeleton, providing the opportunity to discover previously unrecognized interactions between breast cancer cells and bone, including the bone marrow adipose tissue compartment.

A recurring observation during all aspects of our work with these tissues has been the overwhelming presence of adipose tissue within the "red marrow," confirmed by histology, fluorescence microscopy, and the copious production of fat micelles in all culture supernatants. These observations are in keeping with the well-established association between increasing bone marrow adipose with age, which occupies up to 68% of the aging bone marrow compartment (including up to 40% of the red marrow) [26,41,42]). When breast cancer cells were seeded directly onto bone tissue fragments in culture, they routinely migrated into the bone marrow adipose tissue, establishing direct, extended contact with adipocytes. These patterns are consistent with the fact that the human mammary gland is surrounded by a stroma heavily populated by adipose tissue and that adipose tissue is instrumental in directing mammary gland development and primary tumorigenesis [43–47]. Breast cells appear to be exquisitely responsive to the adipose tissue microenvironment, manifested through secreted factors, extracellular matrix components, and cell/cell contacts [45], and studies have shown that these interactions can lead to the emergence of cancer associated adipocytes that promote local tumor progression via stimulation of proliferation, invasion, and angiogenesis [48,49]. As adipose tissue appears to be fundamentally involved in the regulation of breast cell development and tumorigenesis within the mammary gland, it is biologically plausible that breast cancer cells would colonize the bone marrow adipose tissue compartment during metastatic progression. In keeping with breast cancer colonization of the bone marrow adipose tissue, we also observed a strong association between breast cancer cell migration in Transwell assays with increasing levels of the adipokines/cytokines leptin and IL-1β in bone-conditioned medium.

Leptin, an adipokine secreted primarily by adipocytes, regulates satiety and energy balance through receptors located in the hypothalamus. Leptin levels in the blood correlate with body mass index and have been implicated as a link between obesity and numerous pathologies including breast cancer [50–56]. Studies have shown that leptin levels are higher in breast cancer patients than in healthy women, are elevated in obese women with versus without

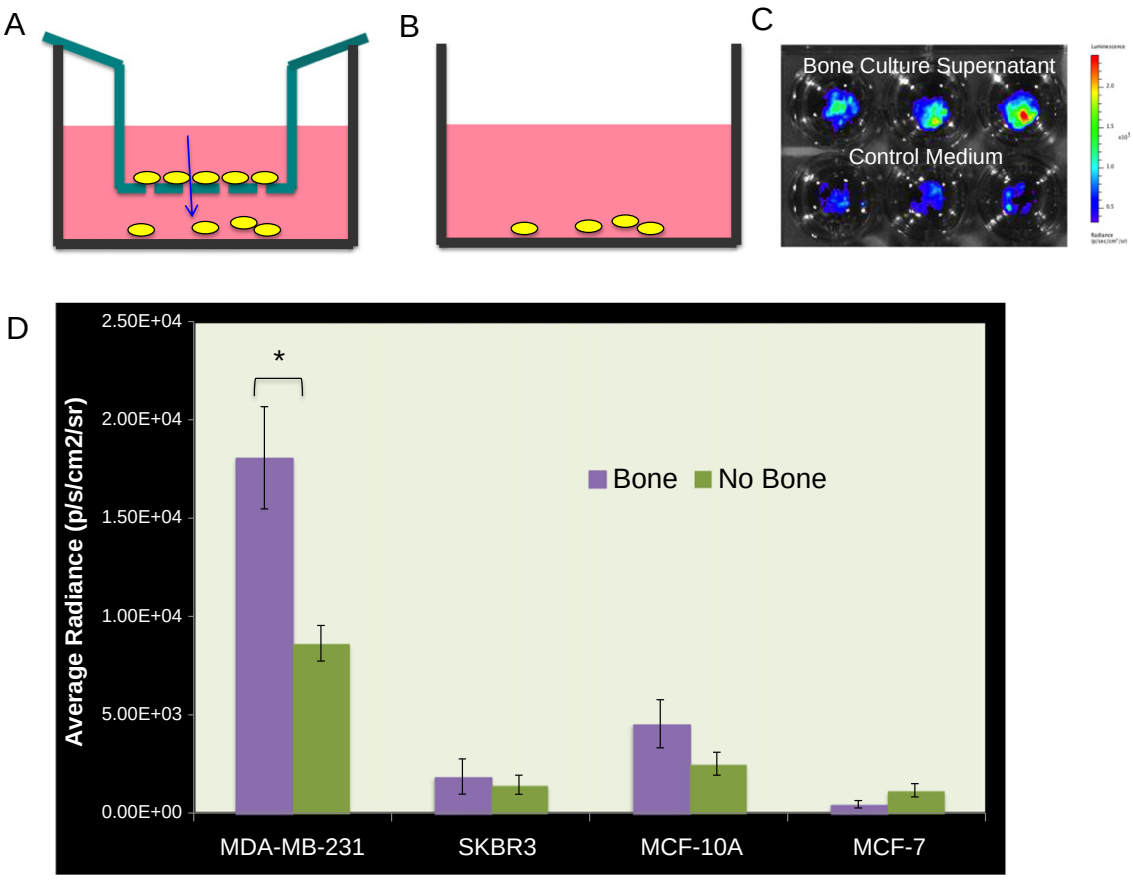


**Figure 4.** Breast cancer cells migrate through microporous membranes to human bone tissue fragment-conditioned medium. (A) Traditional migration assay design showing MDA-MB-231-fLuc-EGFP cells seeded onto the upper surface of an insert with an 8-$\mu$m porous membrane, through which they migrate to into the receiver well containing bone tissue fragment culture supernatant. (B) Postmigration attachment of cells to the bottom of the well. (C) BLI of the receiver plate after removal of the insert following a 20-hour migration period demonstrating enhanced migration of MDA-MB-231-fLuc-EGFP cells into wells containing bone tissue culture supernatant versus control medium (DME-10% FBS). (D) Comparison of migration of four breast cancer cell lines to bone supernatant from THR specimen 61 reveals enhanced migration of MDA-MB-231-fLuc-EGFP cells to bone tissue supernatant versus control medium ($^{*}P < .01$), whereas enhanced migration was not observed for the other three breast cell lines: SKBR3-fLuc-EGFP, MCF-10A-fLuc-EGFP, and MCF-7-fLuc-EGFP.

breast cancer, and correlate with breast tumor size and poor prognosis [52,53,56,57]. In addition, leptin receptors are expressed by breast tumors and correlate with tumor size and poor prognosis in patients with high leptin levels [51,58–60]. In animal models, mammary tumor development is reduced in obese, leptin-deficient versus leptin-intact mice [61]. Numerous *in vitro* studies have shown that leptin promotes the proliferation, migration, and survival of breast cancer cell lines through leptin receptor–activated signaling pathways, including those that regulate the stem cell phenotype and the EMT process [51,62–70].

IL-1β, a pleiotropic cytokine/adipokine produced by a variety of cell types including macrophages, malignant cells, and adipocytes, is widely associated with tumorigenesis and metastatic progression in animal models and is overexpressed in human metastatic tumor tissues [71]. Its secretion by malignant cells and/or the tumor microenvironment has been proposed to fuel tumor-associated inflammation to promote tumor invasiveness through paracrine and autocrine mechanisms [72]. A role in breast cancer cell osteotropism has recently been identified in a mouse model of metastasis where elevated breast cancer cell expression of IL-1β was responsible for MDA-MB-231 breast cancer cell homing to bone [39]. Extension of this study to the analysis of tumor tissues from Stage II/III breast cancer patients demonstrated that patients with IL-1β–positive primary tumors were more likely to develop bone metastases than patients with IL-1β–negative tumors. Although these studies implicate an autocrine mechanism in which breast tumor cell expression drives bone-seeking behavior, our experiments suggest that IL-1β derived from the bone tissue microenvironment also fuels osteotropic breast cancer cell behavior.

As our migration experiments were performed using intact tissues, we did not determine the cellular origin of leptin or IL-1β in bone-conditioned medium. Leptin is secreted primarily by adipose tissues [73,74], and others have reported leptin secretion by isolated bone marrow adipocytes in culture [75]. However, leptin is also secreted in low amounts by other bone cells, including osteoblasts [76,77]. Osteoblasts and adipocytes both originate from mesenchymal stem cells and share some common markers [76]. Although leptin expression by osteoblasts has been reported during the late maturation phase [77], given the size and numbers of adipocytes within the aging bone marrow niche, it is likely that they constitute the predominant source of leptin in the bone-conditioned medium used in our studies.

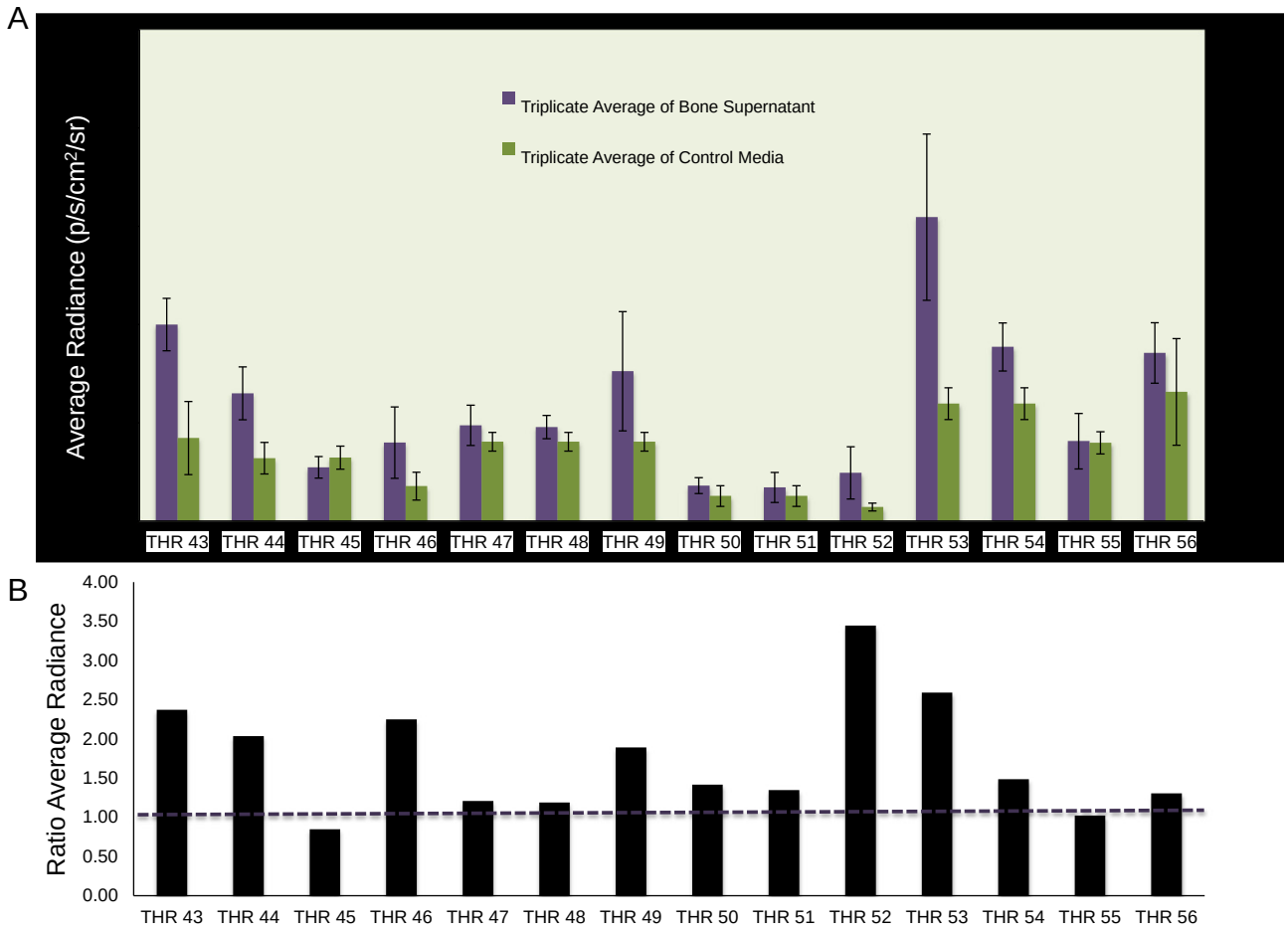


**Figure 5.** MDA-MB-231-fLuc-EGFP breast cancer cell migration is enhanced in the presence of bone tissue-conditioned medium generated from 14 hip replacement surgical specimens. (A) Enhanced migration of MDA-MB-231-fLuc-EGFP cells to bone tissue culture supernatants ($n = 3$) versus control medium ($n = 3$) in experiments performed using bone fragments from 14 THR specimens. (B) Fold increase in migration in the presence of bone-conditioned medium, determined as the ratio of average triplicate BLI signal for migration to bone supernatant over control medium. Overall migration to bone-conditioned medium was significantly greater than to control medium ($P = .0014$).

IL-1β, commonly produced by macrophages during inflammation, is also recognized as an adipokine, and its secretion has been detected in conditioned medium of cultured human preadipocytes, adipocytes, and explanted subcutaneous abdominal adipose tissues [78].

Our observations that breast cancer cells are recruited to human bone tissue-conditioned medium by leptin and IL-1β and colonize the bone marrow adipose tissue compartment of cultured bone tissue fragments are in keeping with an emerging body of work by others demonstrating a seminal role for adipose tissue in fueling ovarian and prostate cancer metastasis [17,28,79,80]. Most ovarian cancers preferentially metastasize to the omentum, an apron-like fold of visceral peritoneum populated by fat cells that extends from the stomach over the lower intestines. Nieman et al. demonstrated that adipocytes promote ovarian cancer cell homing, migration, and invasion of the omentum through the secretion of IL-8, IL-6, MCP-1, and TIMP [79,80]. This work also revealed that during metastatic progression within the omentum, ovarian cancer cells exhibit upregulation of the fatty acid chaperone molecule FABP4, which mediates lipid trafficking and the transfer and uptake of free fatty acids from adipocytes that fuel cancer cell growth. Adipose tissue also appears to be centrally involved in the progression of prostate cancer, which preferentially metastasizes to bone [28]. Using a high-fat diet to induce bone marrow adiposity in a mouse model coupled with *in vitro* studies, Herroon et al. demonstrated that prostate tumors grow faster in a high-fat environment; that lipids are transferred from adipocytes to tumor cells; and that marrow adipocytes fuel the growth and invasiveness of prostate cancer cells by stimulating the upregulation of IL-1β, HMOX-1, and FABP4 [17]. Extending their *in vitro* work to breast cancer cells, this group also reported that MDA-MB-231-BO cells exhibited increased growth and invasiveness in the presence of adipocyte-conditioned medium. Using the same model, Hardaway et al. have demonstrated the role of bone marrow adipose-derived CXCL1 and CXCL2 cytokines in driving the osteolytic process during prostate cancer progression in the skeleton, showing in *in vitro* studies that adipocyte-driven osteoclastogenesis could be reversed through CXCL1 and CXCL2 neutralization. [81]. Their findings are supported by clinical associations implicating an inflammation-driven promotion of progression within the bone that activates the osteolytic cycle. Together, these previously published studies reveal that cancer cells can exploit adipose tissue to thrive during metastasis, providing solid mechanistic evidence that some adipose tissues drive colonization, growth, invasion, and osteolytic processes [17,28,79–81].

A potential role for marrow adipose tissue in breast cancer metastatic progression to bone is also consistent with the established

A

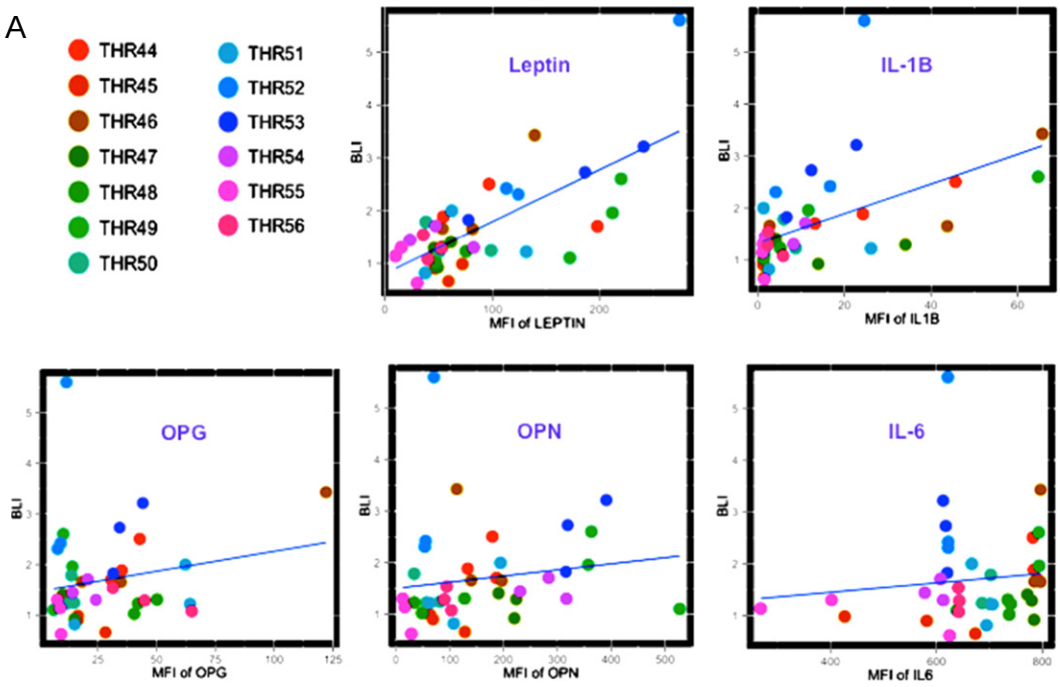


B

| Analyte | Univariate Analysis | | Univariate Analysis | | Multivariate Analysis | |
|---|---|---|---|---|---|---|
| | Coefficient | P-value | Coefficient | P-value | Coefficient | P-value |
| | | | *Adjusted for age and gender* | | | |
| LEPTIN | 0.37764928 | <0.001* | 0.42070464 | <0.001* | 0.29038239 | 0.006* |
| IL1B | 0.21094885 | <0.001* | 0.21492951 | <0.001* | 0.17268468 | 0.001* |
| OPN | 0.10333252 | 0.345 | 0.1002729 | 0.37 | -0.0093809 | 0.891 |
| IL6 | 0.01028457 | 0.981 | -0.0332468 | 0.937 | -0.4851861 | 0.122 |
| OPG | 0.22386902 | 0.045* | 0.21898773 | 0.058 | 0.03323169 | 0.644 |

**Figure 6.** MDA-MB-231-fLuc-EGFP breast cancer cell migration is associated with specific factors present in bone tissue-conditioned medium. (A) Scatter plots illustrating breast cancer cell migration as a function of leptin, IL-1β, OPG, OPN, and IL-6 levels in bone-conditioned medium generated by 13 THR specimens. Triplicate sets of bone-conditioned and control medium for each of the 13 THR specimens were used for migrations assays and MILLIPLEX analysis. Migration, detected by BLI, is plotted on the *Y*-axis, and analyte concentration, expressed as MFI, is plotted on the *X*-axis. (B) Regression analysis of MDA-MB-231-fLuc-EGFP cell migration as a function of analyte levels. Coefficients and *P* values generated by univariate regression analysis (before and after adjustment for age and gender) and multivariate regression analysis (age and gender included as covariates). Breast cancer cell migration was significantly associated with increasing levels of leptin and IL-1β.

association between obesity and poor breast cancer outcomes [82]. One explanation for this association is that local and/or circulating levels of adipokines and cytokines, including leptin, IL-1β, TNF-a, MCP-1, IL6, and IL8, fuel the progression of breast cancer [50,83–86]. This constellation of factors is upregulated during obesity and the associated state of chronic inflammation during which subcutaneous and visceral adipose tissues become heavily infiltrated with immune cells, including macrophages that produce a variety of inflammatory cytokines [83]. However, a recent study did not find a relationship between circulating inflammatory adipokines and breast cancer risk, leading to the suggestion that serum levels of these factors, which tend to signal through paracrine interactions, may not constitute the appropriate surrogate measurement [87]. Our analysis of the human bone secretome suggests that many of these factors are produced in the bone and may signal to breast cancer cells arriving in the bone marrow vasculature to infiltrate and colonize the marrow adipose tissue. Thus, it is possible that cross talk and direct interactions between breast cancer cells and adipose tissue within the microenvironment of the bone may also underlie the association between adipose-associated factors and poor breast cancer outcomes. Future analysis of these mechanisms may therefore lead to improved therapeutic strategies for the management of breast cancer metastasis to bone.

## Conclusions

Our findings in a human bone tissue explant model reveal that breast cancer cells colonize the bone marrow adipose niche and suggest that they are recruited to human bone tissue by leptin and IL-1β. Bone marrow adipose tissue and its molecular signals may be important but understudied components of the breast cancer metastatic niche.

Supplementary data to this article can be found online at http://dx.doi.org/10.1016/j.neo.2015.11.005.

## Contributions

B. L. K. conceived the study. B. L. K., W.-R. L., C. H. C., and Z. S. T. designed experiments. Z. S. T., R. A., M. H. B., and B. L. K. performed experiments. W.-R. L. performed multiplex immunoassay analysis. K. L.

and B. L. K. performed confocal fluorescence microscopy. J. T. and W. W. performed statistical analyses. W. J. M. provided surgical bone tissue specimens. B. L. K., W.-R. L., and W. W. wrote the manuscript.

## Acknowledgements

These studies were funded, in part, by grants from the Alternative Research and Development Foundation (107588), the National Institutes of Health (5R01CA172895-02), and the California Breast Cancer Research Program (201B-0141) and generous support from the Chambers Family Foundation. This work was also supported, in part, by the National Institutes of Health (P30CA124435) using the following Stanford Cancer Institute Shared Resources: Human Immune Monitoring Shared Resource, Cell Sciences Imaging Shared Resource, and Biostatistics and Research Bioinformatics Shared Resource. We thank Drs. Andrew Wilber and R. Scott McIvor for the generous donation of their <pKT2/LuBiG> transposon and pK/hUbiC-SB11 transposase plasmids. We gratefully acknowledge Nancy Bellagamba for facilitating the collection of THR specimens.

## Literature Cited

[1] Coleman RE and Rubens RD (1987). The clinical course of bone metastases from breast cancer. *Br J Cancer* **55**(1), 61–66 [Epub 1987/01/01. PubMed PMID: 3814476].

[2] Mundy GR (2002). Metastasis to bone: causes, consequences and therapeutic opportunities. *Nat Rev Cancer* **2**(8), 584–593. http://dx.doi.org/10.1038/nrc867 [Epub 2002/08/03, PubMed PMID: 12154351].

[3] Paget S (1989). The distribution of secondary growths in cancer of the breast. *Cancer Metastasis Rev* **8**(2), 98–101 [PubMed PMID: 2673568].

[4] Fidler IJ (2003). The pathogenesis of cancer metastasis: the 'seed and soil' hypothesis revisited. *Nat Rev Cancer* **3**(6), 453–458. http://dx.doi.org/10.1038/nrc1098 [PubMed PMID: 12778135].

[5] Mastro AM, Gay CV, and Welch DR (2003). The skeleton as a unique environment for breast cancer cells. *Clin Exp Metastasis* **20**(3), 275–284 [PubMed PMID: 12741685].

[6] Yoneda T (1997). Arterial microvascularization and breast cancer colonization in bone. *Histol Histopathol* **12**(4), 1145–1149 [PubMed PMID: 9302573].

[7] Bersini S, Jeon JS, Dubini G, Arrigoni C, Chung S, Charest JL, Moretti M, and Kamm RD (2014). A microfluidic 3D in vitro model for specificity of breast cancer metastasis to bone. *Biomaterials* **35**(8), 2454–2461. http://dx.doi.org/10.1016/j.biomaterials.2013.11.050 [Epub 2014/01/07, PubMed PMID: 24388382; PMCID: 3905838].

[8] Bussard KM, Venzon DJ, and Mastro AM (2010). Osteoblasts are a major source of inflammatory cytokines in the tumor microenvironment of bone metastatic breast cancer. *J Cell Biochem* **111**(5), 1138–1148. http://dx.doi.org/10.1002/jcb.22799 [Epub 2010/08/05, PubMed PMID: 20683902].

[9] Chen X, Lu J, Ji Y, Hong A, and Xie Q (2014). Cytokines in osteoblast-conditioned medium promote the migration of breast cancer cells. *Tumour Biol* **35**(1), 791–798. http://dx.doi.org/10.1007/s13277-013-1109-0 [PubMed PMID: 24026883].

[10] Jones DH, Nakashima T, Sanchez OH, Kozieradzki I, Komarova SV, Sarosi I, Morony S, Rubin E, Sarao R, and Hojilla CV, et al (2006). Regulation of cancer cell migration and bone metastasis by RANKL. *Nature* **440**(7084), 692–696. http://dx.doi.org/10.1038/nature04524 [PubMed PMID: 16572175].

[11] Kapoor P, Suva LJ, Welch DR, and Donahue HJ (2008). Osteoprotegrin and the bone homing and colonization potential of breast cancer cells. *J Cell Biochem* **103**(1), 30–41. http://dx.doi.org/10.1002/jcb.21382 [PubMed PMID: 17471510].

[12] Koro K, Parkin S, Pohorelic B, Yang AD, Narendran A, Egan C, and Magliocco A (2011). Interactions between breast cancer cells and bone marrow derived cells in vitro define a role for osteopontin in affecting breast cancer cell migration. *Breast Cancer Res Treat* **126**(1), 73–83. http://dx.doi.org/10.1007/s10549-010-0889-9 [Epub 2010/04/20, PubMed PMID: 20401631].

[13] Martinez LM, Vallone VB, Labovsky V, Choi H, Hofer EL, Feldman L, Bordenave RH, Batagelj E, Dimase F, and Villafane AR, et al (2014). Changes in the peripheral blood and bone marrow from untreated advanced breast cancer patients that are associated with the establishment of bone metastases. *Clin Exp Metastasis* **31**(2), 213–232. http://dx.doi.org/10.1007/s10585-013-9622-5 [PubMed PMID: 24173696].

[14] Muller A, Homey B, Soto H, Ge N, Catron D, Buchanan ME, McClanahan T, Murphy E, Yuan W, and Wagner SN, et al (2001). Involvement of chemokine receptors in breast cancer metastasis. *Nature* **410**(6824), 50–56. http://dx.doi.org/10.1038/35065016 [PubMed PMID: 11242036].

[15] Pohorelic B, Singh R, Parkin S, Koro K, Yang AD, Egan C, and Magliocco A (2012). Role of Src in breast cancer cell migration and invasion in a breast cell/bone-derived cell microenvironment. *Breast Cancer Res Treat* **133**(1), 201–214. http://dx.doi.org/10.1007/s10549-011-1753-2 [Epub 2011/09/07, PubMed PMID: 21894461].

[16] Zhang L, Teng Y, Zhang Y, Liu J, Xu L, Qu J, Hou K, Yang X, Liu Y, and Qu X (2012). C-Src-mediated RANKL-induced breast cancer cell migration by activation of the ERK and Akt pathway. *Oncol lett* **3**(2), 395–400. http://dx.doi.org/10.3892/ol.2011.487 [PubMed PMID: 22740919; PMCID: 3362513].

[17] Herroon MK, Rajagurubandara E, Hardaway AL, Powell K, Turchick A, Feldmann D, and Podgorski I (2013). Bone marrow adipocytes promote tumor growth in bone via FABP4-dependent mechanisms. *Oncotarget* **4**(11), 2108–2123 [PubMed PMID: 24240026; PMCID: 3875773].

[18] Shiozawa Y, Eber MR, Berry JE, and Taichman RS (2015). Bone marrow as a metastatic niche for disseminated tumor cells from solid tumors. *BoneKEy rep* **4**, 689. http://dx.doi.org/10.1038/bonekey.2015.57 [PubMed PMID: 26029360; PMCID: 4440229].

[19] Shiozawa Y, Pedersen EA, Havens AM, Jung Y, Mishra A, Joseph J, Kim JK, Patel LR, Ying C, and Ziegler AM, et al (2011). Human prostate cancer metastases target the hematopoietic stem cell niche to establish footholds in mouse bone marrow. *J Clin Invest* **121**(4), 1298–1312. http://dx.doi.org/10.1172/JCI43414 [PubMed PMID: 21436587; PMCID: 3069764].

[20] Ghajar CM, Peinado H, Mori H, Matei IR, Evason KJ, Brazier H, Almeida D, Koller A, Hajjar KA, and Stainier DY, et al (2013). The perivascular niche regulates breast tumour dormancy. *Nat Cell Biol* **15**(7), 807–817. http://dx.doi.org/10.1038/ncb2767 PubMed PMID: 23728425; PMCID: 3826912.

[21] Wang H, Yu C, Gao X, Welte T, Muscarella AM, Tian L, Zhao H, Zhao Z, Du S, and Tao J, et al (2015). The osteogenic niche promotes early-stage bone colonization of disseminated breast cancer cells. *Cancer cell* **27**(2), 193–210. http://dx.doi.org/10.1016/j.ccell.2014.11.017 [PubMed PMID: 25600338; PMCID: 4326554].

[22] Bissell MJ and Radisky D (2001). Putting tumours in context. *Nat Rev Cancer* **1**(1), 46–54. http://dx.doi.org/10.1038/35094059 [Epub 2002/03/20, PubMed PMID: 11900251; PMCID: 2975572].

[23] Joyce JA and Pollard JW (2009). Microenvironmental regulation of metastasis. *Nat Rev Cancer* **9**(4), 239–252. http://dx.doi.org/10.1038/nrc2618 [Epub 2009/03/13, PubMed PMID: 19279573; PMCID: 3251309].

[24] Place AE, Jin Huh S, and Polyak K (2011). The microenvironment in breast cancer progression: biology and implications for treatment. *Breast Cancer Res* **13**(6), 227. http://dx.doi.org/10.1186/bcr2912 [Epub 2011/11/15, PubMed PMID: 22078026; PMCID: 3326543].

[25] Fazeli PK, Horowitz MC, MacDougald OA, Scheller EL, Rodeheffer MS, Rosen CJ, and Klibanski A (2013). Marrow fat and bone–new perspectives. *J Clin Endocrinol Metab* **98**(3), 935–945. http://dx.doi.org/10.1210/jc.2012-3634 [PubMed PMID: 23393168; PMCID: 3590487].

[26] Justesen J, Stenderup K, Ebbesen EN, Mosekilde L, Steiniche T, and Kassem M (2001). Adipocyte tissue volume in bone marrow is increased with aging and in patients with osteoporosis. *Biogerontology* **2**(3), 165–171 [PubMed PMID: 11708718].

[27] Scheller EL and Rosen CJ (2014). What's the matter with MAT? Marrow adipose tissue, metabolism, and skeletal health. *Ann N Y Acad Sci* **1311**, 14–30. http://dx.doi.org/10.1111/nyas.12327 [PubMed PMID: 24650218; PMCID: 4049420].

[28] Hardaway AL, Herroon MK, Rajagurubandara E, and Podgorski I (2014). Bone marrow fat: linking adipocyte-induced inflammation with skeletal metastases. *Cancer Metastasis Rev* **33**(2–3), 527–543. http://dx.doi.org/10.1007/s10555-013-9484-y [Epub 2014/01/09, PubMed PMID: 24398857; PMCID: 4154371].

[29] Contag CH, Lie WR, Bammer MC, Hardy JW, Schmidt TL, Maloney WJ, and King BL (2014). Monitoring dynamic interactions between breast cancer cells and human bone tissue in a co-culture model. *Mol Imaging Biol* **16**(2), 158–166. http://dx.doi.org/10.1007/s11307-013-0685-0 [Epub 2013/09/07, PubMed PMID: 24008275].

[30] Templeton ZS, Bachmann MH, Alluri RV, Maloney WJ, Contag CH, and King BL (2015). Methods for Culturing Human Femur Tissue Explants to Study Breast Cancer Cell Colonization of the Metastatic Niche. *J Vis Exp* **97**(e52656), 1–10. http://dx.doi.org/10.3791/52656.

[31] Multhaup M, Karlen AD, Swanson DL, Wilber A, Somia NV, Cowan MJ, and McIvor RS (2010). Cytotoxicity associated with artemis overexpression after lentiviral vector-mediated gene transfer. *Hum Gene Ther* **21**(7), 865–875. http://dx.doi.org/10.1089/hum.2009.162 [Epub 2010/02/19, 162. PubMed PMID: 20163250; PMCID: 2938362].

[32] Thorne SH, Barak Y, Liang W, Bachmann MH, Rao J, Contag CH, and Matin A (2009). CNOB/ChrR6, a new prodrug enzyme cancer chemotherapy. *Mol Cancer Ther* **8**(2), 333–341 [Epub 2009/02/05. doi: 1535–7163. MCT-08-0707 [pii] 10.1158/1535-7163.MCT-08-0707. PubMed PMID: 19190118].

[33] Liu X, Ory V, Chapman S, Yuan H, Albanese C, Kallakury B, Timofeeva OA, Nealon C, Dakic A, and Simic V, et al (2012). ROCK inhibitor and feeder cells induce the conditional reprogramming of epithelial cells. *Am J Pathol* **180**(2), 599–607. http://dx.doi.org/10.1016/j.ajpath.2011.10.036 [Epub 2011/12/23, PubMed PMID: 22189618; PMCID: 3349876].

[34] Rosenberg-Hasson Y, Hansmann L, Liedtke M, Herschmann I, and Maecker HT (2014). Effects of serum and plasma matrices on multiplex immunoassays. *Immunol Res* **58**(2–3), 224–233. http://dx.doi.org/10.1007/s12026-014-8491-6 [PubMed PMID: 24522699; PMCID: 4332596].

[35] Johansson JU, Pradhan S, Lokteva LA, Woodling NS, Ko N, Brown HD, Wang Q, Loh C, Cekanaviciute E, and Buckwalter M, et al (2013). Suppression of inflammation with conditional deletion of the prostaglandin E2 EP2 receptor in macrophages and brain microglia. *J Neurosci* **33**(40), 16016–16032. http://dx.doi.org/10.1523/JNEUROSCI.2203-13.2013 [PubMed PMID: 24089506; PMCID: 3787507].

[36] Team RC (2012). R: A language and environment for statistical computing. Foundation for Statistical Computing.

[37] Bates DM, Maechler M, and Bolker B (2012). lmme4: Linear mixed-effects models using S4 classes. R package version 0.999999-0.

[38] Kim IS and Baek SH (2010). Mouse models for breast cancer metastasis. *Biochem Biophys Res Commun* **394**(3), 443–447. http://dx.doi.org/10.1016/j.bbrc.2010.03.070 [Epub 2010/03/17, PubMed PMID: 20230796].

[39] Nutter F, Holen I, Brown HK, Cross SS, Evans CA, Walker M, Coleman RE, Westbrook JA, Selby PJ, and Brown JE, et al (2014). Different molecular profiles are associated with breast cancer cell homing compared with colonisation of bone: evidence using a novel bone-seeking cell line. *Endocr Relat Cancer* **21**(2), 327–341. http://dx.doi.org/10.1530/ERC-13-0158 [PubMed PMID: 24413608].

[40] Riccio AI, Wodajo FM, and Malawer M (2007). Metastatic carcinoma of the long bones. *Am Fam Physician* **76**(10), 1489–1494 [Epub 2007/12/07, PubMed PMID: 18052014].

[41] Vande Berg BC, Malghem J, Lecouvet FE, and Maldague B (1998). Magnetic resonance imaging of normal bone marrow. *Eur Radiol* **8**(8), 1327–1334. http://dx.doi.org/10.1007/s003300050547 [PubMed PMID: 9853209].

[42] Hwang S and Panicek DM (2007). Magnetic resonance imaging of bone marrow in oncology, Part 1. *Skeletal Radiol* **36**(10), 913–920. http://dx.doi.org/10.1007/s00256-007-0309-3 [PubMed PMID: 17492443].

[43] Wiseman BS and Werb Z (2002). Stromal effects on mammary gland development and breast cancer. *Science* **296**(5570), 1046–1049. http://dx.doi.org/10.1126/science.1067431 [PubMed PMID: 12004111; PMCID: 2788989].

[44] Gnerlich JL, Yao KA, Fitchev PS, Goldschmidt RA, Bond MC, Cornwell M, and Crawford SE (2013). Peritumoral expression of adipokines and fatty acids in breast cancer. *Ann Surg Oncol* **20**(Suppl 3), S731–S738. http://dx.doi.org/10.1245/s10434-013-3274-1 [PubMed PMID: 24052317].

[45] Iyengar P, Combs TP, Shah SJ, Gouon-Evans V, Pollard JW, Albanese C, Flanagan L, Tenniswood MP, Guha C, and Lisanti MP, et al (2003). Adipocyte-secreted factors synergistically promote mammary tumorigenesis through induction of anti-apoptotic transcriptional programs and proto-oncogene stabilization. *Oncogene* **22**(41), 6408–6423. http://dx.doi.org/10.1038/sj.onc.1206737 [PubMed PMID: 14508521].

[46] Liu E, Samad F, and Mueller BM (2013). Local adipocytes enable estrogen-dependent breast cancer growth: Role of leptin and aromatase. *Adipocyte* **2**(3), 165–169. http://dx.doi.org/10.4161/adip.23645 [PubMed PMID: 23991363; PMCID: 3756105].

[47] Landskroner-Eiger S, Park J, Israel D, Pollard JW, and Scherer PE (2010). Morphogenesis of the developing mammary gland: stage-dependent impact of adipocytes. *Dev Biol* **344**(2), 968–978. http://dx.doi.org/10.1016/j.ydbio.2010.06.019 [PubMed PMID: 20599899; PMCID: 2917626].

[48] Dirat B, Bochet L, Dabek M, Daviaud D, Dauvillier S, Majed B, Wang YY, Meulle A, Salles B, and Le Gonidec S, et al (2011). Cancer-associated adipocytes exhibit an activated phenotype and contribute to breast cancer invasion. *Cancer Res* **71**(7), 2455–2465. http://dx.doi.org/10.1158/0008-5472.CAN-10-3323 [PubMed PMID: 21459803].

[49] Park J, Morley TS, Kim M, Clegg DJ, and Scherer PE (2014). Obesity and cancer–mechanisms underlying tumour progression and recurrence. *Nat Rev Endocrinol* **10**(8), 455–465. http://dx.doi.org/10.1038/nrendo.2014.94 [PubMed PMID: 24935119; PMCID: 4374431].

[50] Khan S, Shukla S, Sinha S, and Meeran SM (2013). Role of adipokines and cytokines in obesity-associated breast cancer: therapeutic targets. *Cytokine Growth Factor Rev* **24**(6), 503–513. http://dx.doi.org/10.1016/j.cytogfr.2013.10.001 [PubMed PMID: 24210902].

[51] Garcia-Robles MJ, Segura-Ortega JE, and Fafutis-Morris M (2013). The biology of leptin and its implications in breast cancer: a general view. *J Interferon Cytokine Res* **33**(12), 717–727. http://dx.doi.org/10.1089/jir.2012.0168 [Epub 2013/07/23, PubMed PMID: 23869900].

[52] Niu J, Jiang L, Guo W, Shao L, Liu Y, and Wang L (2013). The Association between Leptin Level and Breast Cancer: A Meta-Analysis. *PloS one* **8**(6), e67349. http://dx.doi.org/10.1371/journal.pone.0067349 [PubMed PMID: 23826274; PMCID: 3694967].

[53] Saxena NK and Sharma D (2013). Multifaceted leptin network: the molecular connection between obesity and breast cancer. *J Mammary Gland Biol Neoplasia* **18**(3–4), 309–320. http://dx.doi.org/10.1007/s10911-013-9308-2 [PubMed PMID: 24214584].

[54] Schmidt S, Monk JM, Robinson LE, and Mourtzakis M (2015). The integrative role of leptin, oestrogen and the insulin family in obesity-associated breast cancer: potential effects of exercise. *Obes Rev* **16**(6), 473–487. http://dx.doi.org/10.1111/obr.12281 [PubMed PMID: 25875578].

[55] Ando S, Barone I, Giordano C, Bonofiglio D, and Catalano S (2014). The Multifaceted Mechanism of Leptin Signaling within Tumor Microenvironment in Driving Breast Cancer Growth and Progression. *Front oncol* **4**, 340. http://dx.doi.org/10.3389/fonc.2014.00340 [PubMed PMID: 25505738; PMCID: 4245002].

[56] Romero-Figueroa Mdel S, Garduno-Garcia Jde J, Duarte-Mote J, Matute-Gonzalez G, Gomez-Villanueva A, and De la Cruz-Vargas J (2013). Insulin and leptin levels in obese patients with and without breast cancer. *Clin Breast Cancer* **13**(6), 482–485. http://dx.doi.org/10.1016/j.clbc.2013.08.001 [Epub 2013/10/03, PubMed PMID: 24084031].

[57] Delort L, Rossary A, Farges MC, Vasson MP, and Caldefie-Chezet F (2015). Leptin, adipocytes and breast cancer: Focus on inflammation and anti-tumor immunity. *Life Sci* **140**, 37–48. http://dx.doi.org/10.1016/j.lfs.2015.04.012 [PubMed PMID: 25957709].

[58] Garofalo C, Koda M, Cascio S, Sulkowska M, Kanczuga-Koda L, Golaszewska J, Russo A, Sulkowski S, and Surmacz E (2006). Increased expression of leptin and the leptin receptor as a marker of breast cancer progression: possible role of obesity-related stimuli. *Clin Cancer Res* **12**(5), 1447–1453. http://dx.doi.org/10.1158/1078-0432.CCR-05-1913 [Epub 2006/03/15, PubMed PMID: 16533767].

[59] Ishikawa M, Kitayama J, and Nagawa H (2004). Enhanced expression of leptin and leptin receptor (OB-R) in human breast cancer. *Clin Cancer Res* **10**(13), 4325–4331. http://dx.doi.org/10.1158/1078-0432.CCR-03-0749 [PubMed PMID: 15240518].

[60] Miyoshi Y, Funahashi T, Tanaka S, Taguchi T, Tamaki Y, Shimomura I, and Noguchi S (2006). High expression of leptin receptor mRNA in breast cancer tissue predicts poor prognosis for patients with high, but not low, serum leptin levels. *Int J Cancer* **118**(6), 1414–1419. http://dx.doi.org/10.1002/ijc.21543 [PubMed PMID: 16206269].

[61] Zheng Q, Dunlap SM, Zhu J, Downs-Kelly E, Rich J, Hursting SD, Berger NA, and Reizes O (2011). Leptin deficiency suppresses MMTV-Wnt-1 mammary tumor growth in obese mice and abrogates tumor initiating cell survival. *Endocr Relat Cancer* **18**(4), 491–503. http://dx.doi.org/10.1530/ERC-11-0102 [Epub 2011/06/04, PubMed PMID: 21636700; PMCID: 3197719].

[62] Dieudonne MN, Machinal-Quelin F, Serazin-Leroy V, Leneveu MC, Pecquery R, and Giudicelli Y (2002). Leptin mediates a proliferative response in human MCF7 breast cancer cells. *Biochem Biophys Res Commun* **293**(1), 622–628. http:

//dx.doi.org/10.1016/S0006-291X(02)00205-X [Epub 2002/06/11, PubMed PMID: 12054648].

[63] Fusco R, Galgani M, Procaccini C, Franco R, Pirozzi G, Fucci L, Laccetti P, and Matarese G (2010). Cellular and molecular crosstalk between leptin receptor and estrogen receptor-{alpha} in breast cancer: molecular basis for a novel therapeutic setting. *Endocr Relat Cancer* **17**(2), 373–382. http://dx.doi.org/10.1677/ERC-09-0340 [Epub 2010/04/23, PubMed PMID:20410173].

[64] Ray A, Nkhata KJ, and Cleary MP (2007). Effects of leptin on human breast cancer cell lines in relationship to estrogen receptor and HER2 status. *Int J Oncol* **30**(6), 1499–1509 [Epub 2007/05/10, PubMed PMID:17487372].

[65] Yuan HJ, Sun KW, and Yu K (2014). Leptin promotes the proliferation and migration of human breast cancer through the extracellular-signal regulated kinase pathway. *Mol Med Rep* **9**(1), 350–354. http://dx.doi.org/10.3892/mmr.2013.1786 [Epub 2013/11/12, PubMed PMID: 24213635].

[66] Strong AL, Ohlstein JF, Biagas BA, Rhodes LV, Pei DT, Tucker HA, Llamas C, Bowles AC, Dutreil MF, and Zhang S, et al (2015). Leptin produced by obese adipose stromal/stem cells enhances proliferation and metastasis of estrogen receptor positive breast cancers. *Breast Cancer Res* **17**, 112. http://dx.doi.org/10.1186/s13058-015-0622-z [PubMed PMID: 26286584; PMCID: 4541745].

[67] Dubois V, Jarde T, Delort L, Billard H, Bernard-Gallon D, Berger E, Geloen A, Vasson MP, and Caldefie-Chezet F (2014). Leptin induces a proliferative response in breast cancer cells but not in normal breast cells. *Nutr Cancer* **66**(4), 645–655. http://dx.doi.org/10.1080/01635581.2014.894104 [Epub 2014/04/18, PubMed PMID: 24738610].

[68] Kim SH, Nagalingam A, Saxena NK, Singh SV, and Sharma D (2011). Benzyl isothiocyanate inhibits oncogenic actions of leptin in human breast cancer cells by suppressing activation of signal transducer and activator of transcription 3. *Carcinogenesis* **32**(3), 359–367. http://dx.doi.org/10.1093/carcin/bgq267 [PubMed PMID: 21163886; PMCID: 3105585].

[69] Wang L, Tang C, Cao H, Li K, Pang X, Zhong L, Dang W, Tang H, Huang Y, and Wei L, et al (2015). Activation of IL-8 via PI3K/Akt-dependent pathway is involved in leptin-mediated epithelial-mesenchymal transition in human breast cancer cells. *Cancer Biol Ther* **16**(8), 1220–1230. http://dx.doi.org/10.1080/15384047.2015.1056409 [PubMed PMID: 26121010].

[70] Wolfson B, Eades G, and Zhou Q (2015). Adipocyte activation of cancer stem cell signaling in breast cancer. *World J Biol Chem* **6**(2), 39–47. http://dx.doi.org/10.4331/wjbc.v6.i2.39 [PubMed PMID: 26009703; PMCID: 4436905].

[71] Elaraj DM, Weinreich DM, Varghese S, Puhlmann M, Hewitt SM, Carroll NM, Feldman ED, Turner EM, and Alexander HR (2006). The role of interleukin 1 in growth and metastasis of human cancer xenografts. *Clin Cancer Res* **12**(4), 1088–1096. http://dx.doi.org/10.1158/1078-0432.CCR-05-1603 [PubMed PMID: 16489061].

[72] Apte RN, Krelin Y, Song X, Dotan S, Recih E, Elkabets M, Carmi Y, Dvorkin T, White RM, and Gayvoronsky L, et al (2006). Effects of micro-environment- and malignant cell-derived interleukin-1 in carcinogenesis, tumour invasiveness and tumour-host interactions. *Eur J Cancer* **42**(6), 751–759. http://dx.doi.org/10.1016/j.ejca.2006.01.010 [PubMed PMID: 16530403].

[73] Margetic S, Gazzola C, Pegg GG, and Hill RA (2002). Leptin: a review of its peripheral actions and interactions. *Int J Obes Relat Metab Disord* **26**(11), 1407–1433. http://dx.doi.org/10.1038/sj.ijo.0802142 [PubMed PMID: 12439643].

[74] Masuzaki H, Ogawa Y, Isse N, Satoh N, Okazaki T, Shigemoto M, Mori K, Tamura N, Hosoda K, and Yoshimasa Y, et al (1995). Human obese gene expression. Adipocyte-specific expression and regional differences in the adipose tissue. *Diabetes* **44**(7), 855–858 [PubMed PMID: 7789654].

[75] Laharrague P, Larrouy D, Fontanilles AM, Truel N, Campfield A, Tenenbaum R, Galitzky J, Corberand JX, Penicaud L, and Casteilla L (1998). High expression of leptin by human bone marrow adipocytes in primary culture. *FASEB J* **12**(9), 747–752 [PubMed PMID: 9619453].

[76] Kollmer M, Buhrman JS, Zhang Y, and Gemeinhart RA (2013). Markers Are Shared Between Adipogenic and Osteogenic Differentiated Mesenchymal Stem Cells. *J Dev Biol Tissue Eng* **5**(2), 18–25. http://dx.doi.org/10.5897/JDBTE2013.0065 [PubMed PMID: 24013643; PMCID: 3765027].

[77] Reseland JE, Syversen U, Bakke I, Qvigstad G, Eide LG, Hjertner O, Gordeladze JO, and Drevon CA (2001). Leptin is expressed in and secreted from primary cultures of human osteoblasts and promotes bone mineralization. *J Bone Miner Res* **16**(8), 1426–1433. http://dx.doi.org/10.1359/jbmr.2001.16.8.1426 [PubMed PMID: 11499865].

[78] Schipper HS, de Jager W, van Dijk ME, Meerding J, Zelissen PM, Adan RA, Prakken BJ, and Kalkhoven E (2010). A multiplex immunoassay for human adipokine profiling. *Clin Chem* **56**(8), 1320–1328. http://dx.doi.org/10.1373/-clinchem.2010.146118 [PubMed PMID: 20530731].

[79] Nieman KM, Kenny HA, Penicka CV, Ladanyi A, Buell-Gutbrod R, Zillhardt MR, Romero IL, Carey MS, Mills GB, and Hotamisligil GS, et al (2011). Adipocytes promote ovarian cancer metastasis and provide energy for rapid tumor growth. *Nat Med* **17**(11), 1498–1503. http://dx.doi.org/10.1038/nm.2492 [PubMed PMID: 22037646; PMCID: 4157349].

[80] Nieman KM, Romero IL, Van Houten B, and Lengyel E (2013). Adipose tissue and adipocytes support tumorigenesis and metastasis. *Biochim Biophys Acta* **1831**(10), 1533–1541. http://dx.doi.org/10.1016/j.bbalip.2013.02.010 [Epub 2013/03/19, PubMed PMID: 23500888; PMCID: 3742583].

[81] Hardaway AL, Herroon MK, Rajagurubandara E, and Podgorski I (2015). Marrow adipocyte-derived CXCL1 and CXCL2 contribute to osteolysis in metastatic prostate cancer. *Clin Exp Metastasis* **32**(4), 353–368. http://dx.doi.org/10.1007/s10585-015-9714-5 [PubMed PMID: 25802102; PMCID: 4393805].

[82] Ford NA, Devlin KL, Lashinger LM, and Hursting SD (2013). Deconvoluting the obesity and breast cancer link: secretome, soil and seed interactions. *J Mammary Gland Biol Neoplasia* **18**(3–4), 267–275. http://dx.doi.org/10.1007/s10911-013-9301-9 [Epub 2013/10/05, PubMed PMID: 24091864; PMCID: 3874287].

[83] Howe LR, Subbaramaiah K, Hudis CA, and Dannenberg AJ (2013). Molecular pathways: adipose inflammation as a mediator of obesity-associated cancer. *Clin Cancer Res* **19**(22), 6074–6083. http://dx.doi.org/10.1158/1078-0432 [Epub 2013/08/21, PubMed PMID: 23958744; PMCID: 3891839].

[84] Gross AL, Newschaffer CJ, Hoffman-Bolton J, Rifai N, and Visvanathan K (2013). Adipocytokines, inflammation, and breast cancer risk in postmenopausal women: a prospective study. *Cancer Epidemiol Biomarkers Prev* **22**(7), 1319–1324. http://dx.doi.org/10.1158/1055-9965.EPI-12-1444 PubMed PMID: 23651666; PMCID: 4417498.

[85] Cho YA, Sung MK, Yeon JY, Ro J, and Kim J (2013). Prognostic role of interleukin-6, interleukin-8, and leptin levels according to breast cancer subtype. *Cancer Res Treat* **45**(3), 210–219. http://dx.doi.org/10.4143/crt.2013.45.3.210 [PubMed PMID: 24155680; PMCID: 3804733].

[86] Khandekar MJ, Cohen P, and Spiegelman BM (2011). Molecular mechanisms of cancer development in obesity. *Nat Rev Cancer* **11**(12), 886–895. http://dx.doi.org/10.1038/nrc3174 [PubMed PMID: 22113164].

[87] Gunter MJ, Wang T, Cushman M, Xue X, Wassertheil-Smoller S, Strickler HD, Rohan TE, Manson JE, McTiernan A, and Kaplan RC, et al (2015). Circulating Adipokines and Inflammatory Markers and Postmenopausal Breast Cancer Risk. *J Natl Cancer Inst* **107**(9). http://dx.doi.org/10.1093/jnci/djv169 [PubMed PMID: 26185195].